

# The He(I), threshold photoelectron and constant ion state spectroscopy of vinylchloride (C<sub>2</sub>H<sub>3</sub>Cl)

R. Locht<sup>a</sup>, B. Leyh<sup>a,1</sup>, K. Hottmann<sup>b</sup>, H. Baumgärtel<sup>b</sup>

<sup>a</sup> *Département de Chimie Générale et de Chimie Physique, Institut de Chimie, Bât. B6c, Université de Liège, Sart-Tilman par B-4000 Liège 1, Belgium*

<sup>b</sup> *Institut für Physikalische und Theoretische Chemie, Freie Universität Berlin, Takustraße 3, D-14195 Berlin, Germany*

## Abstract

Using synchrotron radiation, the threshold photoelectron (TPES) spectrum of C<sub>2</sub>H<sub>3</sub>Cl and constant ion state (CIS) spectroscopy of C<sub>2</sub>H<sub>3</sub>Cl, are reported. For comparison, the He(I) photoelectron spectrum has also been measured and reexamined. The threshold photoelectron spectrum has been measured between 9.0 and 25.0 eV, and the photon energy range of 9.9-12.0 eV has been investigated in detail. Many features have been identified and tentatively assigned with the help of the photoabsorption spectroscopic results [1]. These data were compared with a well-resolved He(I) photoelectron spectrum. The fine structure observed in the two first ionic states is assigned to progressions belonging partially to previously unobserved vibration normal modes. State-selected CIS spectra have been recorded for the first vibronic states between 10.0 and 11.67 eV. They exhibit fine structure assigned to autoionization of Rydberg states.

## 1. Introduction.

In the framework of our program aiming at the detailed examination of the ionization and the dissociation dynamics of isolated and clustered mono- and di-substituted ethylenes, we were in a first step interested in extending the spectroscopic data related to these compounds by investigating the photoabsorption spectrum [1], the threshold photoelectron spectrum (TPES) and the constant ion state (CIS) spectra of vinylchloride.

The vinylchloride molecule has been thoroughly investigated by Kaufel [2] through dissociative photoionization mass spectrometry in almost all important decay channels. For several fragmentation paths, Tornow [3] studied the dissociative electroionization of C<sub>2</sub>H<sub>3</sub>Cl together with the fragment ion translational energy. The He(I) photoelectron spectrum of this molecule is well known, though recorded at medium resolution [4]. The threshold photoelectron spectrum and the CIS spectra of the C<sub>2</sub>H<sub>3</sub>Cl<sup>+</sup> vibronic states are not available to our knowledge.

In this paper we report about the threshold photoelectron spectrum and the CIS spectra of the first vibronic states of C<sub>2</sub>H<sub>3</sub>Cl. For comparison, the He(I) photoelectron spectrum obtained under medium- and high-resolution conditions will also be reported.

## 2. Experimental

The experimental setup, and more specifically the electron energy analyzer used in these experiments will be described and discussed in detail in a forthcoming paper [5]. Only the most salient features will be described, and for the sake of clarity, the three experimental techniques used in the present experiments will be laid out in more detail in this section.

In all experiments reported here we used the vacuum UV light from the synchrotron radiation provided by the electron storage ring BESSY (Berlin). This light is dispersed by a 3 m normal incidence monochromator (3 m-NIM-1 line) equipped with a 2400 l/mm Pt-grating. The entrance and exit slit widths were set at 50 to 200  $\mu$ m depending on the signal intensity. Owing to the second-order contribution at low photon energy, LiF or MgF<sub>2</sub> windows were used in the 8.0-11.8 eV and 8.0-10.8 eV ranges, respectively. The photon energy scale of the monochromator is calibrated with rare gas photoabsorption and/or threshold photoelectron spectra to reach an accuracy better than 2-3 meV. For this purpose, usually Ar and sometimes Xe are used.

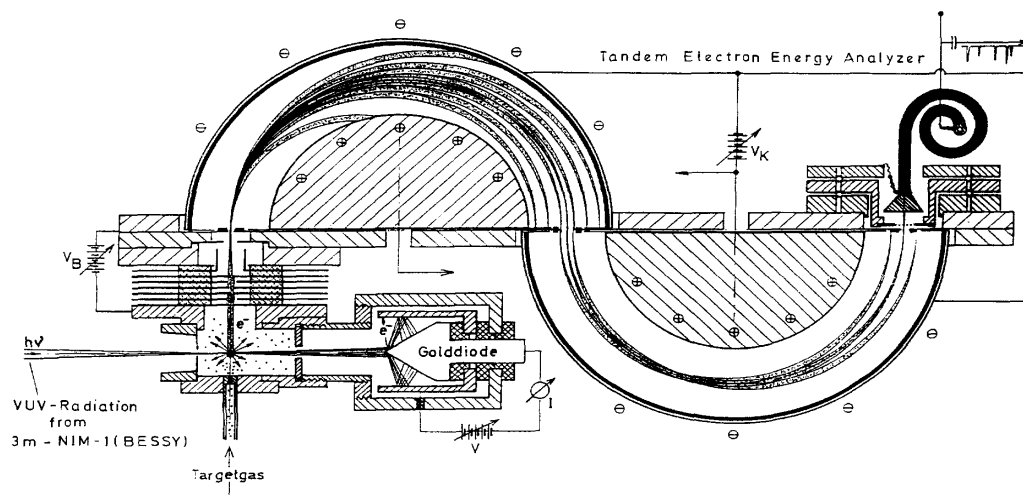
The light beam is focussed into an ion chamber, in the focussing plane of a tandem electron spectrometer consisting in two 180° electrostatic deflectors as shown in Fig. 1. This spectrometer is working at constant energy resolution, i.e. at constant pass energy  $E_0$  defined by potential  $V_K$ . The energy resolution at full width at half maximum (FWHM) is given by  $\Delta E/E_0 = w/4R_0 = w/104$ , where  $w$  and  $R_0$  are the slit width and the radius of the sector field, respectively expressed in millimeters. In the experiments reported in this paper, slit widths of 0.5 and 1.0 mm and pass energies of 1 up to 10 eV have been used. FWHM of less than 10 meV have

---

<sup>1</sup> Chercheur qualifié du F.N.R.S. Belgium.

been achieved in He(I) and threshold photoelectron spectra.

**Fig. 1.** Experimental setup used in this work showing: (1) the ionization chamber; (2) the gold diode; and (3) the different parts of the tandem electron spectrometer.



In addition to the synchrotron storage ring beam-current, the photoelectron signal of a gold diode, inserted in the ion chamber, at the opposite of the 3 m-NIM monochromator exit slit, is measured in order to normalize the photoabsorption spectra and the photoelectron signals in the TPES and CIS spectra.

The most obvious operating mode of this experimental setup is the measurement of 'constant wavelength' photoelectron spectra. Optimal resolution being obtained at low  $V_R$  values,  $V_B$  is scanned and the ionizing radiation wavelength is kept constant.

The second operating mode is the measurement of 'constant photoelectron energy' spectra. These are recorded by tuning the photon energy  $h\nu$  and keeping constant the energy  $E_{kin}^e$  of the photoelectrons transmitted through the tandem electron energy analyzers system. This transmitted photoelectron energy  $E_{kin}^e$  is given by the difference  $e(V_B - V_K)$  (see Fig. 1). More specifically, the electron energy analyzers can be run under conditions where  $V_B \approx V_K$ , transmitting only 'zero-kinetic energy' or 'threshold' (TPES) photoelectrons. This equality is optimized for highest threshold photoelectron signal intensity. This fine tuning allows us to take contact potentials into account.

The threshold photoelectron spectrum of the sample gas has to be normalized to the photon transmission function of the monochromator by measuring the photoelectron current intensity of a gold diode (see Fig. 1).

The third kind of experiments performed with this instrument is the constant ion state (CIS) spectroscopy of vibrational and/or electronic states of molecular ions [6]. The aim of this measurement is to examine the relative partial ionization cross-sections as a function of the photon energy for well-defined electronic and/or vibrational states of the molecular ion under investigation. The existence of autoionization phenomena strongly perturbs the photoionization and dissociative photoionization cross-sections by inducing dramatic variations in the distributions in the final ionic states.

For running a CIS spectrum of a preselected vibronic level of the molecular ion, one needs to keep the energy difference  $h\nu - E_{kin}^e = IE$  constant, i.e. the ionization energy corresponding to the considered ionic state. This requires that the photon energy  $h\nu$  and the photoelectron kinetic energy  $E_{kin}^e$  be scanned in parallel.

For this purpose the electron spectrometer is first optimized for threshold photoelectrons where  $h\nu = IE$  at a preset analyzer pass energy  $eV_R$  and for which  $V_B = V_R$  is adjusted. By increasing the photon energy by a magnitude  $\Delta(h\nu)$ , the photoelectron kinetic energy is increased by  $\Delta E_{kin}^e = \Delta(h\nu)$  and is given by  $eV_B + \Delta E_{kin}^e$ . These defocussed electrons could only be transmitted through the electron spectrometer by applying a voltage  $V_B - \Delta E_{kin}^e$  to compensate the defocussing energy increment  $\Delta E_{kin}^e$ . This is achieved by applying a  $-\Delta V_B$  steplike ramp on  $V_B$ , increasing synchronously with the photon energy scan.

To obtain the relative partial photoionization cross-section, the CIS curve obtained by the way described above has to be normalized for the transmission functions of: (1) the photon energy monochromator and (2) the electron energy analyzer. The former is recorded simultaneously with the CIS spectrum whereas the latter function is obtained by recording the normalized CIS curve of a rare gas, e.g.  $Ar^+ (^2P_{1/2})$  exhibiting no

structure over the same electron energy range as for the investigated molecular ion.

The  $C_2H_3Cl$  sample used in these experiments, purchased from Linde A.G. (99% purity), is introduced without further purification. The ultimate vacuum in the ionization chamber is about  $10^{-8}$  mbar. Unless otherwise stated, the 3 m NIM monochromator entrance and exit slit widths are 200  $\mu m$  for the present experiment. The electron spectrometers have slit widths of 0.5 mm and pass energies  $V_R = 10$  and 5 eV are used for medium- and high-resolution purposes in TPES spectroscopy. The former pass energy is used throughout when CIS spectra are recorded.

### 3. Experimental results

For the easiness of the discussion and for the sake of clarity, the He(I), the threshold and the CIS spectra will be presented and discussed separately.

#### 3.1. The threshold and He(I) photoelectron spectra

The threshold photoelectron spectrum of  $C_2H_3Cl$  has been investigated over a wide photon energy range, i.e. 9.0-30.0 eV. The upper limit is fixed by the grating transmission function. The electron spectrometer has been adjusted for medium-resolution conditions, i.e. 5 eV pass energy allowing 25 meV resolution. Fig. 2a shows the spectrum extending up to 25 eV photon energy. No electron signal is observed above this ionization energy.

Eight well-defined bands are observed at vertical energies of  $10.013 \pm 0.005$ ,  $11.672 \pm 0.005$ ,  $13.18 \pm 0.01$ ,  $13.51 \pm 0.01$ ,  $15.34 \pm 0.01$ ,  $16.28 \pm 0.01$ ,  $18.767 \pm 0.005$  and at  $\sim 22.8$  eV. In addition to these major features, weak and sharp structures have to be mentioned between 10.7 and 11.6 eV whereas (a) diffuse band(s) is (are) obviously present and buried in the 11.6 and 13.18 eV bands.

For comparison the He(I) photoelectron spectrum of  $C_2H_3Cl$  has been recorded over the whole ionization energy range available and at medium resolution (25 meV) and is shown in Fig. 2b. The energy scale of this spectrum has been calibrated with respect to six ionization energies in the photoelectron spectrum of an Ar/Kr/Xe mixture. Except for the two first bands exhibiting sharp and intense features, the four most energetic bands look more diffuse and continuous. The present observation agree with those reported earlier [4,7-9] as shown in Table 1.

Two remarkable differences between the TPES-and the He(I) photoelectron spectra have to be mentioned. First, the presence in the former spectrum of additional structures such as the weak and sharp features between 10.7 and 11.6 eV and the broad continuum-shaped bands buried in the 11.6 and 13.18 eV bands. These have to be ascribed to resonant excitation of the TPES spectrum. The second important difference between the two spectra are the dramatic differences of ionization cross-sections of the different ionic states. Referring to the first ionic excited state, the He(I) photoelectron spectrum is dominated by the first excited state and the five other bands exhibit about the same intensity whereas in the TPES spectrum the ionization bands observed between 13.18 and 16.28 eV are clearly predominant. For a closer examination of the low-energy side of the TPES spectrum, a high-resolution (10 meV) scan of this energy range has been performed. The result is shown in Fig. 3a. For comparison a He(I) photoelectron spectrum has been recorded in the same energy range with the same resolution and is displayed in Fig. 3b. This figure clearly shows in the TPES spectrum: (1) the presence of the sharp but weak structures in the 10.7-11.6 eV photon energy range and (2) an underlying, slightly modulated continuum buried in the second band. All these features are absent in the He(I) spectrum. Very clear are also the drastic differences of relative intensities of the individual structures.

**Table 1** Comparison between the vertical ionization energies (eV) of  $C_2H_3Cl$  as obtained by using He(I), He(II) and threshold photoelectron spectroscopy

State	He(I)/He(II)					TPES
	[4]	[7]	[8]	[9]	this work	this work
$\tilde{X} 2a'^{-1}$	10.15	10.18	10.2	10.16	10.005(5)	10.013(5)
$\tilde{A} 7a'^{-1}$	11.61	11.72	11.7	11.64	11.664(5)	11.672(5)
$\tilde{B} 1a'^{-1}$	13.07	13.14	13.2	13.10	13.13(2)	13.18(2)
$\tilde{C} 6a'^{-1}$	13.55	13.56	13.6	13.60	13.56(2)	13.51(2)
$\tilde{D} 5a'^{-1}$	15.40	15.39	15.4	15.40	15.35(2)	15.34(2)
$\tilde{E} 4a'^{-1}$	16.30	16.31	16.3	16.40	16.29(2)	16.28(2)
$\tilde{F} 3a'^{-1}$	18.95	18.76	19.0	18.80	18.741(20)	18.767(5)
$\tilde{G}2a'^{-1}$	-	-	$\approx 23$	23	-	-

The figure in parentheses represents one standard deviation.

**Fig. 2.** Medium-resolution (a) threshold photoelectron spectrum of  $C_2H_3Cl$  recorded between 9.0 and 25.0 eV photon energy and (b) He(I) photoelectron spectrum of  $C_2H_3Cl$  obtained between 9.0 and 20.0 eV.

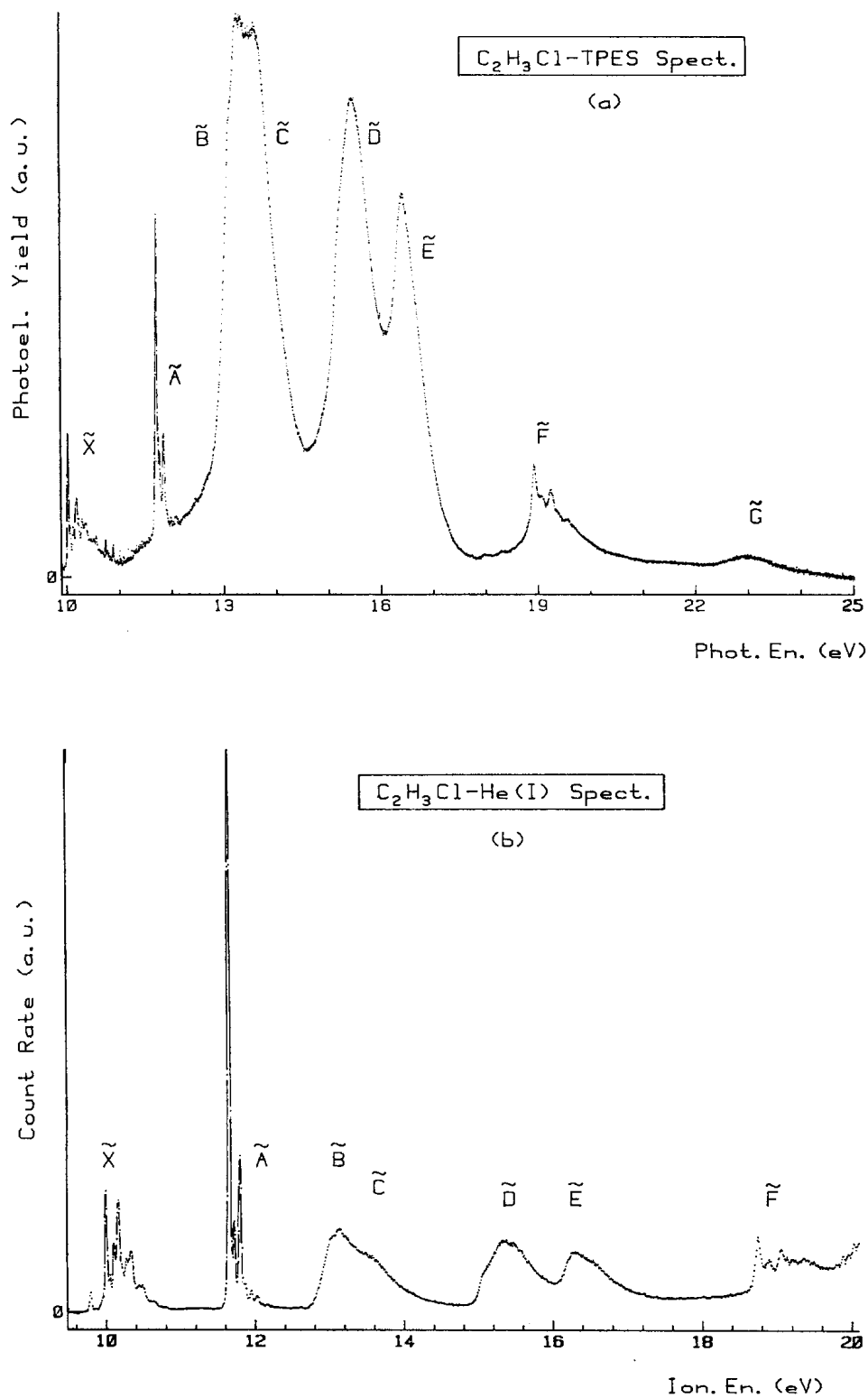


**Fig. 3.** High-resolution (a) threshold photoelectron spectrum and (b) He(I) photoelectron spectrum of  $C_2H_3Cl$  recorded between 9.0 and 12.0 eV photon energy.

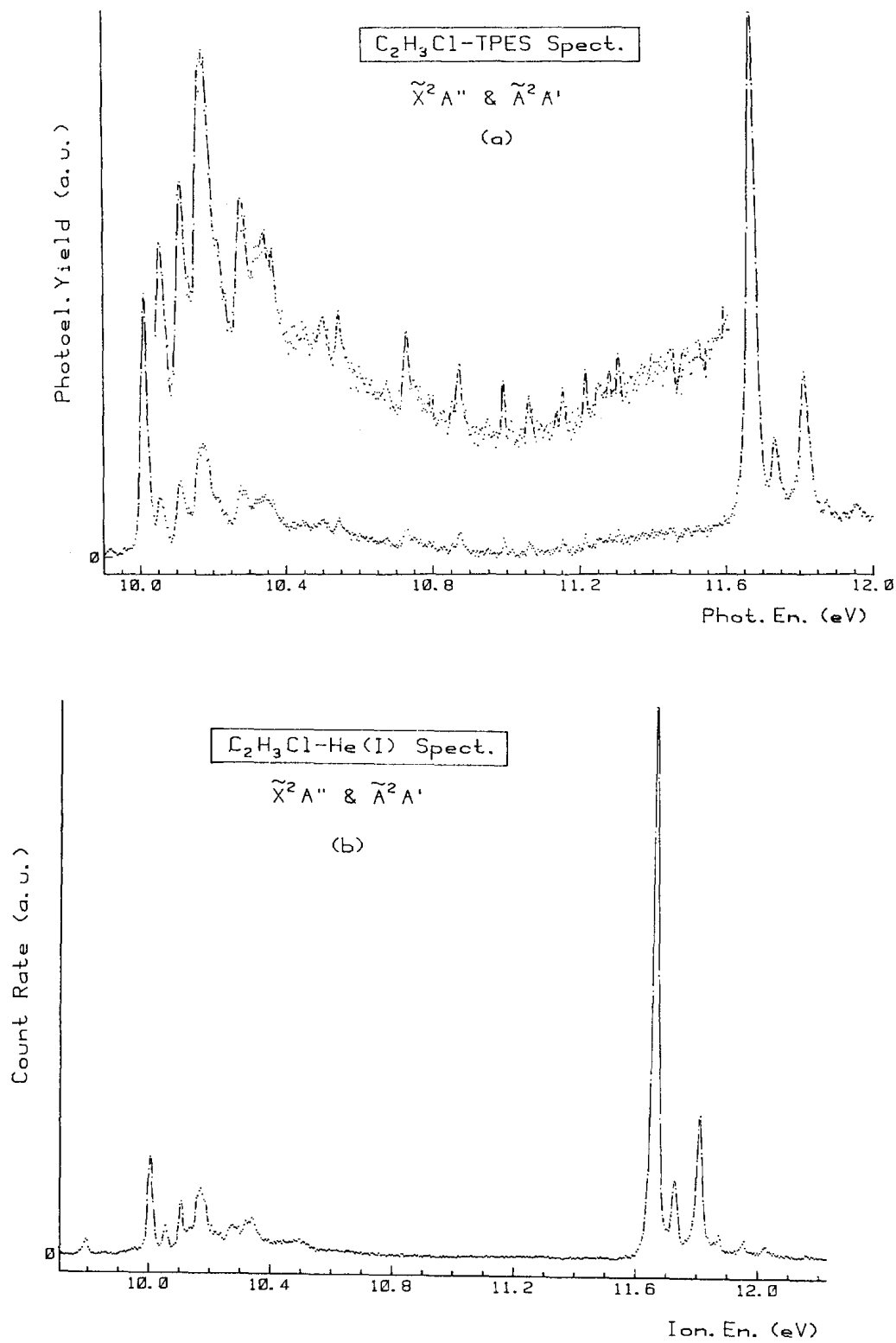


**Fig. 4.** CIS spectra noticed from (a) to (f), corresponding to specified vibrational levels of  $\text{C}_2\text{H}_3\text{Cl}^+$  in the  $\tilde{X}^2A''$  and  $\tilde{A}^2A'$  states, at indicated photon energy.

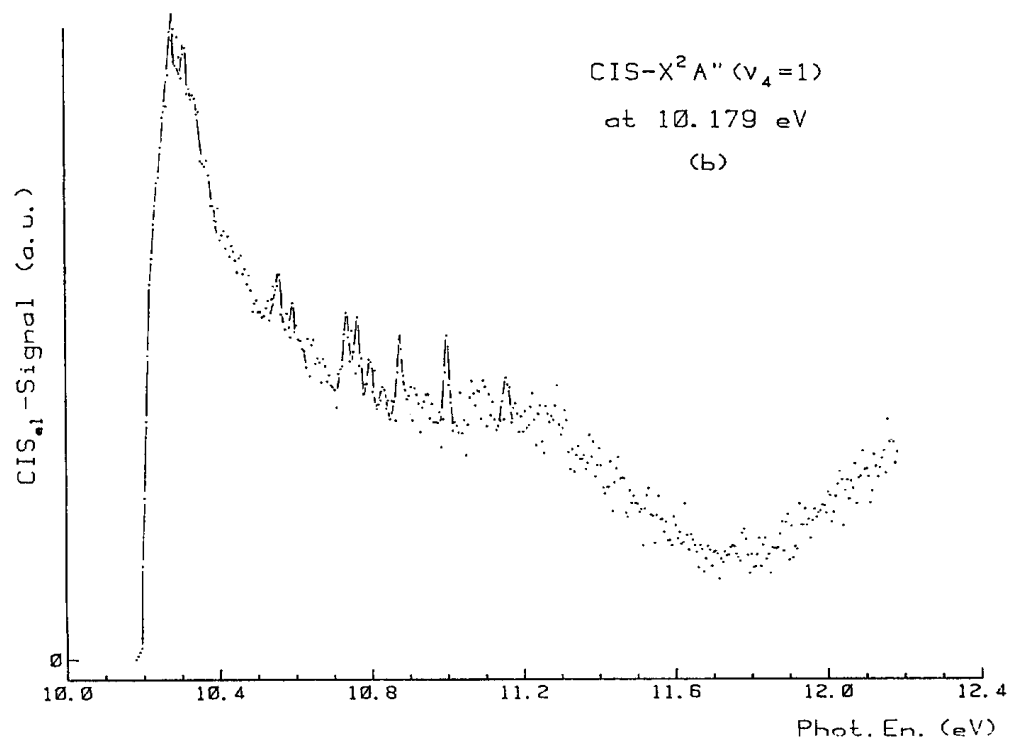
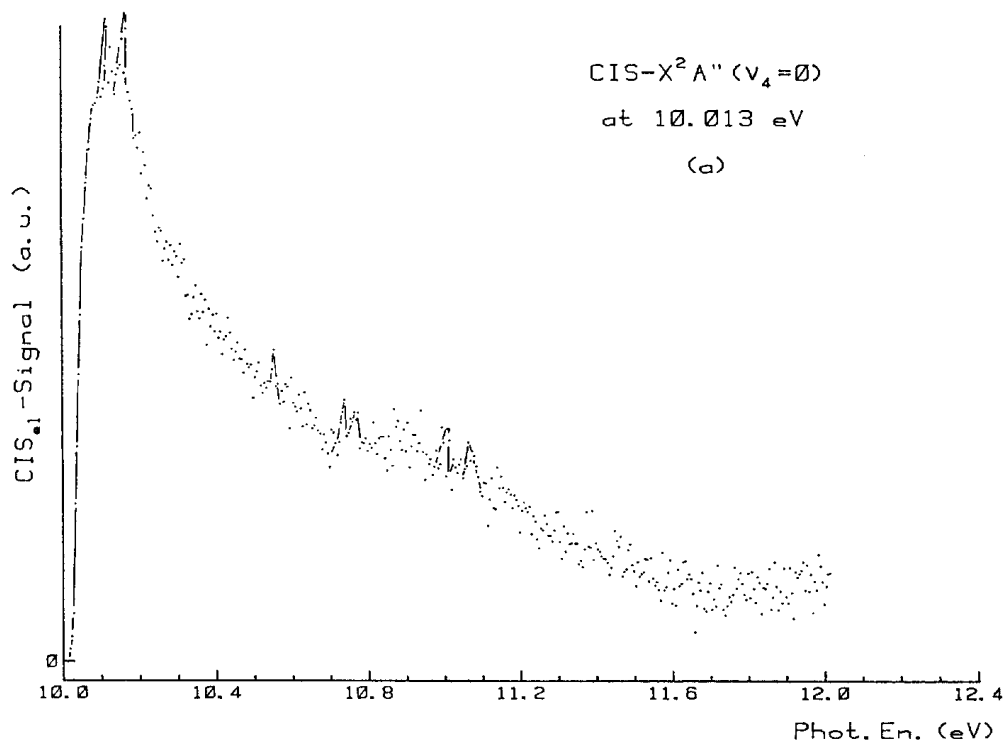


**Fig. 4** (continued).

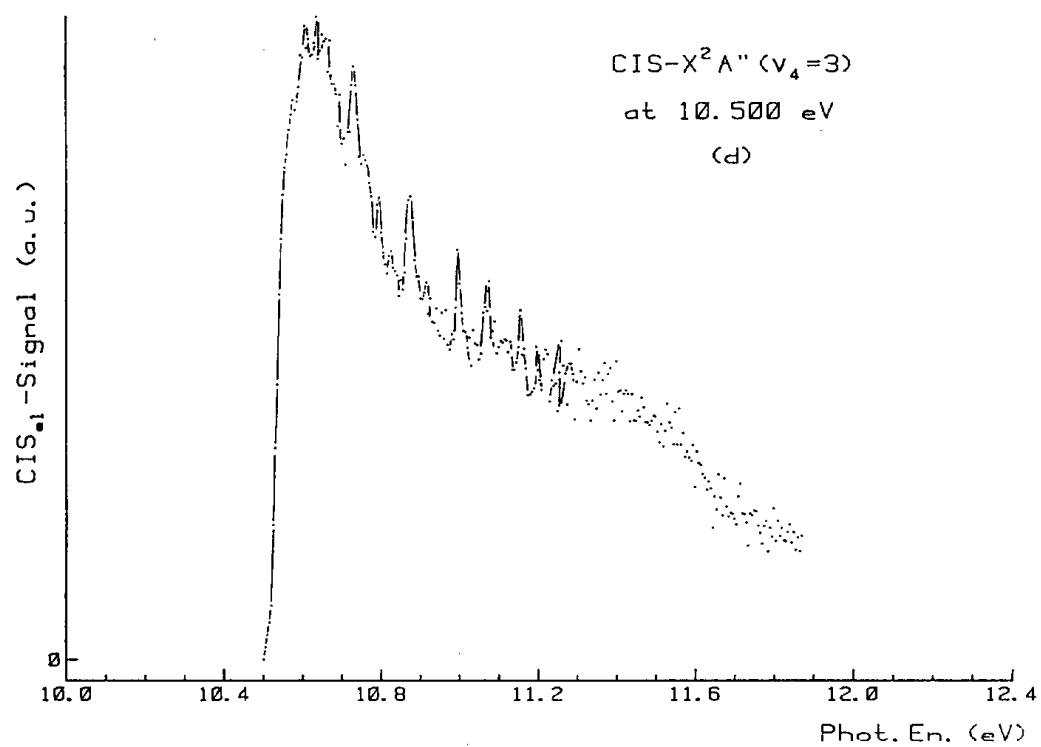
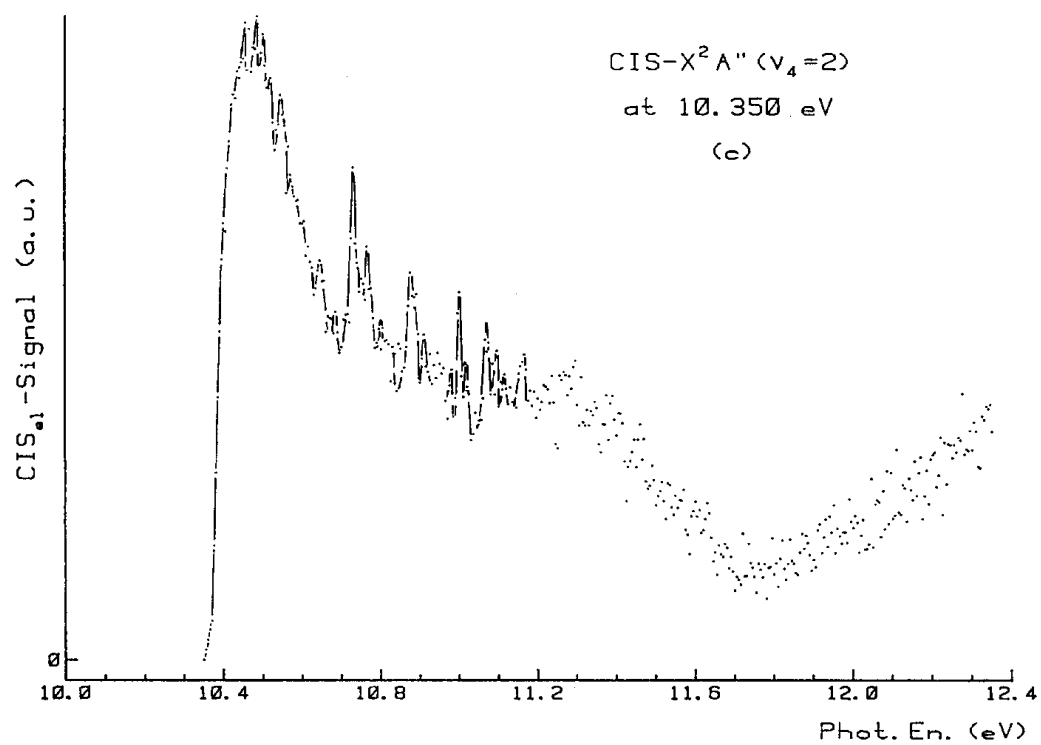


**Fig. 4** (continued).

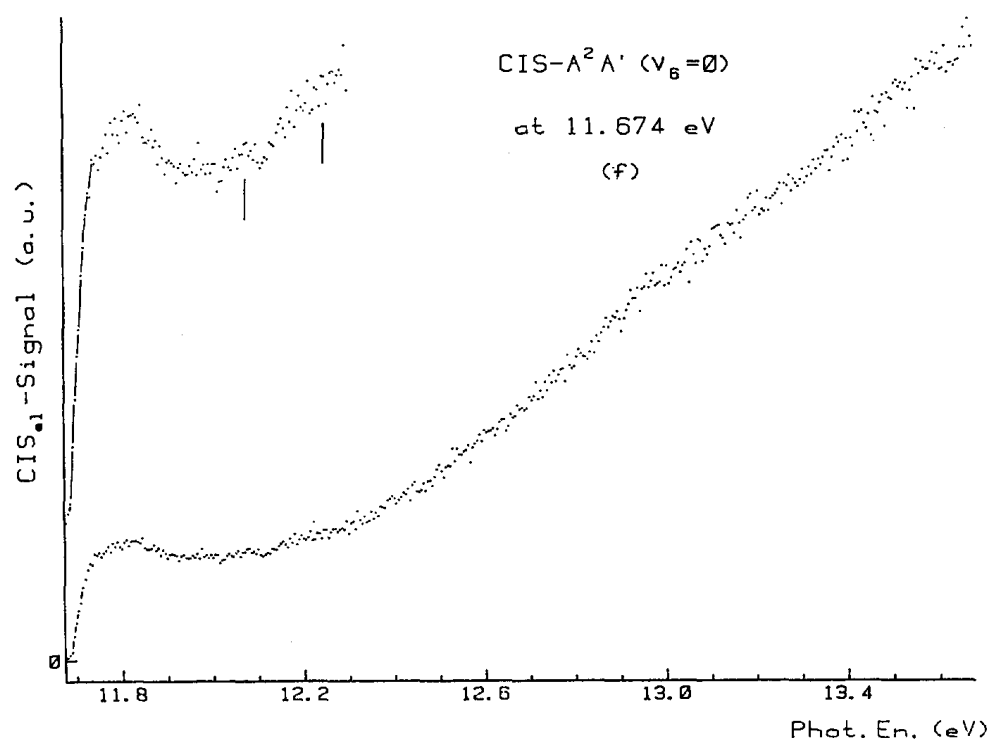
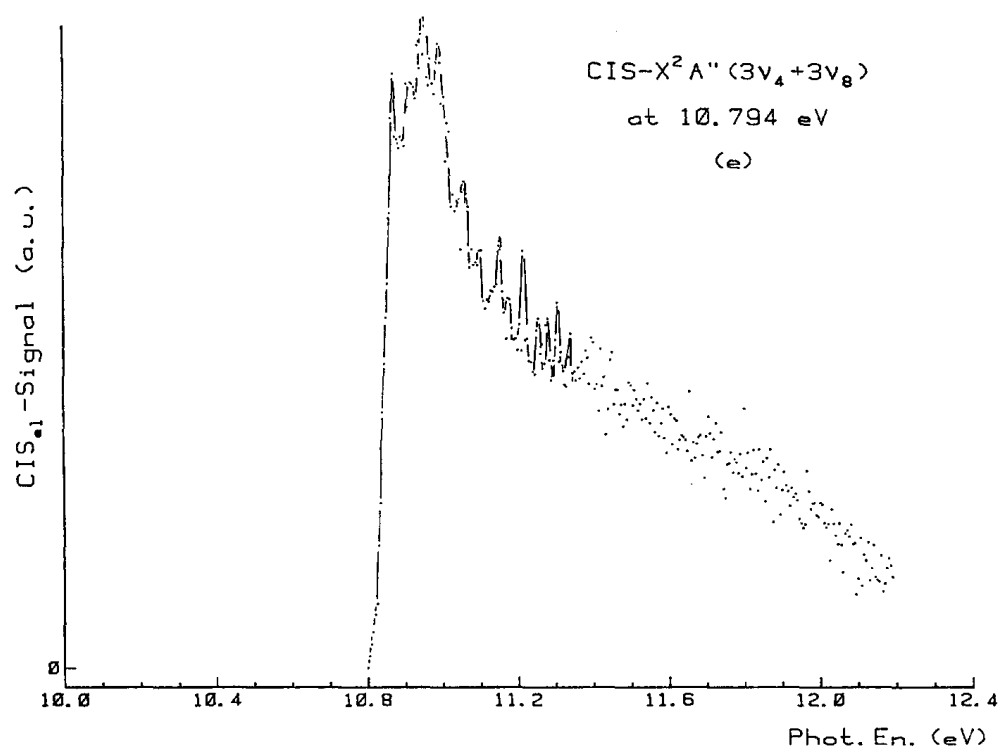
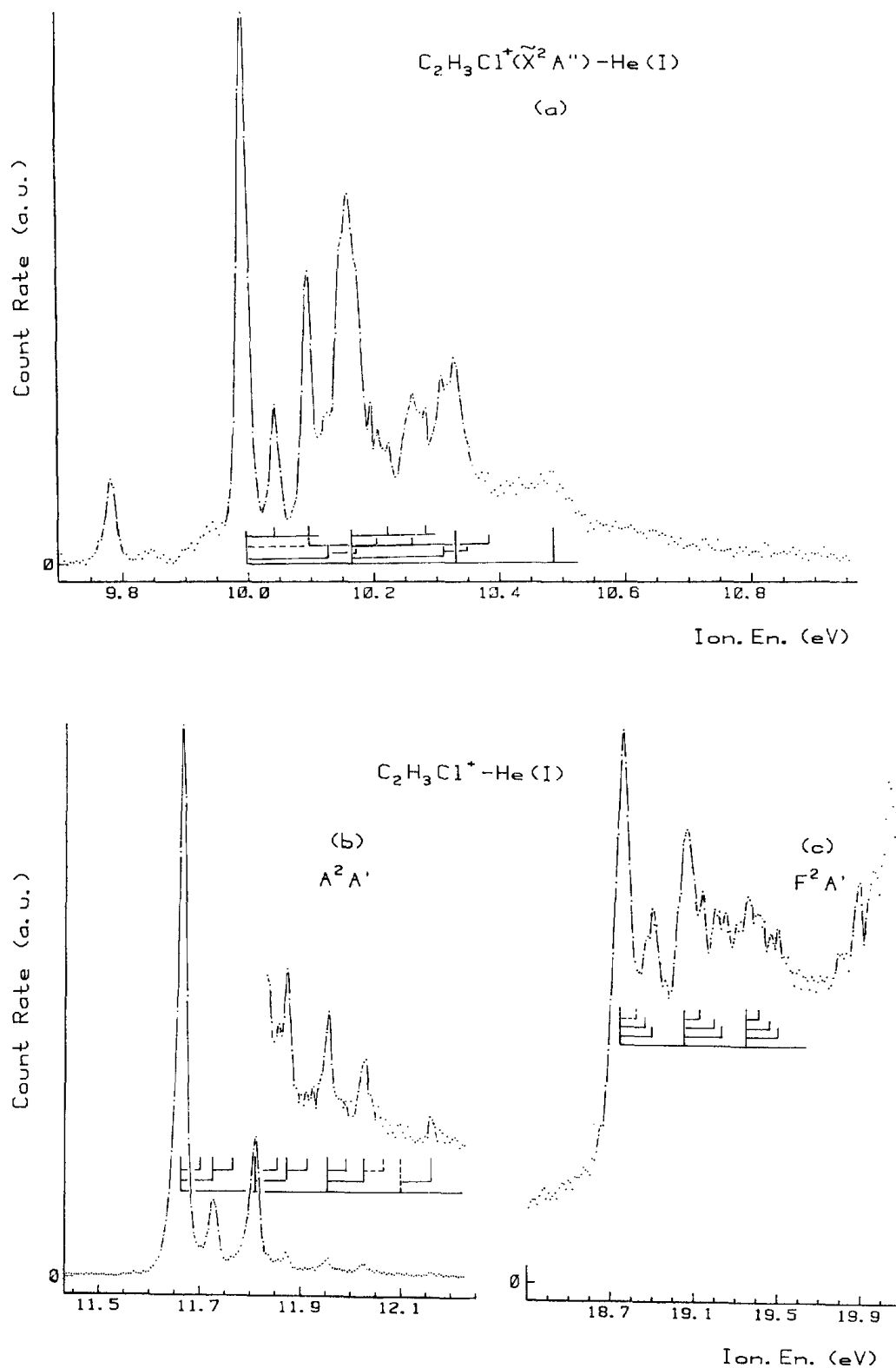




**Fig. 5.** Extended energy scale photoelectron spectrum of: (a) the  $\tilde{X}^2A''$  state; (b) the  $\tilde{A}^2A'$  state; and (c) the  $\tilde{F}^2A'$  state of  $C_2H_3Cl^+$  showing the detail of the vibrational fine structure of these three bands.



### 3.2. The constant ion state spectra

The CIS spectra were recorded in the energy range of the structured region covered by the  $\tilde{X}^2A''$  and  $\tilde{A}^2A'$  of  $C_2H_3Cl$ . Owing to the weakness of the signal in this photon energy range, these time consuming measurements were restricted to the most intense features in the TPES spectrum, i.e. on the first four vibrational levels of the major  $\nu_4$  progression in the  $\tilde{X}^2A''$  state and the vibrationless level of the  $\tilde{A}^2A'$  state. These are shown in Fig. 4a-f. Only one measurement has been performed in the 'fine structured' region, i.e. at 10.800 eV.

A first examination of these CIS spectra clearly shows a quite different shape of these curves. The CIS spectra corresponding to the vibrationless level of both the  $\tilde{X}^2A''$  state and the  $\tilde{A}^2A'$  state show a smooth decrease without any detectable structure up to 12.0 eV. Contrarily, the CIS spectra corresponding to the  $\nu = 1$  to  $\nu = 3$  of the  $\nu_4$  progression in the  $\tilde{X}^2A''$  state exhibit sharp structures superimposed on a continuous background. The intensity of these features regularly increases with increasing vibrational quantum number. Several CIS curves show a marked dip at about 11.8 eV followed by a fairly rapid increase. This peculiarity is not observed in the CIS spectrum related to the vibrationless level of the  $\tilde{X}^2A''$  state. The CIS curve of the vibrationless level of the  $\tilde{A}^2A'$  state exhibits a shallow minimum at about 12.1 eV and then continuously increases with increasing photon energy, at least up to 13.7 eV.

## 4. Discussion

### 4.1. The photoelectron spectra of $C_2H_3Cl$

#### 4.1.1. The He(I) photoelectron spectrum

In terms of molecular orbital description, restricted to the valence and inner-valence orbitals, the electronic structure of the  $C_2H_3Cl$  molecule in its ground electronic state ( $C_s$  symmetry) could be represented by [8]:

$$(1a')^2 (2a')^2 (3a')^2 (4a')^2 (5a')^2 (6a')^2 (1a'')^2 \\ \times (7a')^2 (2a'')^2 \tilde{X}^1A'$$

The medium-resolution photoelectron spectrum shown in Fig. 3b is in good agreement with previous observations [4,7-9]. As already mentioned, this spectrum is dominated by the sharp and intense feature at 11.664 eV. Except the two first bands, all other features are almost structureless. The adiabatic or vertical ionization energies measured in the present work are listed in Table 1. Very good agreement is found with previously reported data [4,7-9]. However, a discrepancy has to be mentioned for the lowest ionization energy. In the present work a value of  $10.005 \pm 0.010$  eV is obtained and is markedly lower than earlier determinations ranging from 10.15 to 10.20 eV. Rydberg series analyses from our work (see preceding paper [1]) and photoionization mass spectrometry [10] strongly favour an ionization energy of  $10.00 \pm 0.01$  eV.

Three bands, corresponding respectively to the ground electronic state  $\tilde{X}^2A''$ , to the first electronic excited state  $\tilde{A}^2A'$  and to the sixth electronic excited state  $\tilde{F}^2A'$ , show a more or less extended vibrational structure. The first two states were investigated at higher resolution, i.e. with an electron analyzer pass energy of 410 meV. The  $Xe^+(^2P_{1/2})$  peak is characterized by a FWHM = 12 meV under these conditions. Fig. 5a and b displays the results for the two first photoelectron bands.

Fig. 5a shows the first ionic band obtained with these conditions and the energies of all observed features are listed in Table 2. The accuracy is better than 5 meV but the precision is limited by the energy interval between two adjacent data points which is 5 meV. The low-energy signal at 9.795 eV has to be assigned to the ionization energy of the  $\tilde{A}^2A'$  state with the He(I)- $\beta$  line at 53.7 nm or 23.088 eV. As displayed in Fig. 5a and listed in Table 2, the fine structure observed in the  $\tilde{X}^2A''$  state of the  $C_2H_3Cl^+$  ion has been assigned to vibrational progressions involving four vibrational normal modes, i.e.  $\omega_4 = 1320 \pm 70$   $cm^{-1}$  corresponding to the C=C valence and  $CH_2$  scissoring mode,  $\omega_7 = 1130 \pm 60$   $cm^{-1}$  involving the H-CC-H deformation mode,  $\omega_8 = 820 \pm 20$   $cm^{-1}$  corresponding to the  $CH_2$  rocking and C-Cl stretching mode and  $\omega_9 = 430 \pm 40$   $cm^{-1}$  implying the  $CH_2$  rocking mode. These data are averaged values and the error is given by the maximum deviation from the average which takes into account the precision on the energy measurements. As mentioned earlier [1], an MNDO analysis [11] of the vibrational modes led to wavenumbers of  $\omega_4 = 1533$   $cm^{-1}$ ,  $\omega_7 = 1085$   $cm^{-1}$ ,  $\omega_8 = 889$   $cm^{-1}$  and  $\omega_9 = 377$   $cm^{-1}$  in the ground electronic state of  $C_2H_3Cl^+$ .

The features of the fine structure observed in the second band are clearly shown in Fig. 5b and their energies are listed in Table 2. The proposed assignments are inserted in the same figure. Three normal vibrational modes could be considered and these are characterized by the wavenumbers  $\omega_6 = 1160 \pm 20$   $cm^{-1}$ ,  $\omega_8 = 520 \pm 30$   $cm^{-1}$  and  $\omega_9 = 300 \pm 50$   $cm^{-1}$  successively. The corresponding wavenumbers in the ground state of the

neutral molecule are  $\omega_6 = 1279 \text{ cm}^{-1}$  (HCC1 scissoring),  $\omega_8 = 720 \text{ cm}^{-1}$  ( $\text{CH}_2$  rocking and C-Cl stretching) and  $\omega_9 = 395 \text{ cm}^{-1}$  ( $\text{CH}_2$  rocking) [11]. By the 7a' [the in-plane p(Cl) or  $p_{||}$  lone pair orbital] [8] ionization the  $\omega_6$  normal vibrational mode is only slightly modified (by about 10%) whereas both the  $\omega_8$  and  $\omega_9$  normal modes undergo a more significant lowering of about 25% or more. These latter vibrations share a  $\text{CH}_2$  rocking vibration which seem to be subjected to the strongest modification. The 7a' molecular orbital should thus have a fairly strong bonding character with respect to the geminal  $\text{CH}_2$  group.

**Table 2** Energy levels (eV) and tentative assignment (0 means vibration-less level and predicted energy in eV) of the fine structure observed in the He(I)- and TPES photoelectron spectra of the  $\text{C}_2\text{H}_3\text{Cl}^+$  ( $\tilde{X}^2A'$ ,  $\tilde{A}^2A'$  and  $\tilde{F}^2A'$ ) states

He(I)	TPES	Absorp.	Assignment
10.005	10.013	-	0
10.054	10.056	10.065	$\nu_9$
10.108	10.107	-	$2\nu_9$
-	10.113	10.117	$\nu_8$
10.138	-	-	$\nu_7$
10.158	10.164	-	$3\nu_9$
10.172	10.173	-	$\nu_4$
10.187	10.188	10.180	$\nu_7 + \nu_9$
10.217	10.215	10.216	$2\nu_8$ (10.219)
10.236	-	-	$\nu_4 + \nu_9$
10.276	10.278	-	$\nu_4 + \nu_8$
10.286	10.290	-	$\nu_4 + 2 \nu_9$
-	-	10.305	
10.320	-	-	$\nu_4 + \nu_7$
10.342	10.350	-	$2\nu_4$ (10.339)
10.362	-	-	$\nu_4 + \nu_7 + \nu_9$
10.394	10.392	-	$\nu_4 + 2\nu_8$ (10.381)
-	10.449	-	$2\nu_4 + \nu_8$ (10.441)
10.497	10.500	10.510	$3\nu_4$ (10.501)
-	10.545	10.549	$2\nu_4 + 2\nu_8$ (10.543)
-	10.602	10.602	$3 \nu_4 + \nu_8$ (10.603)
-	10.677	10.686	$4\nu_4$ (10.663)
-	10.730	10.731	$3\nu_4 + 2\nu_8$ (10.705)
-	10.760	10.761	$4\nu_4 + \nu_8$ (10.765)
-	10.794	10.798	$3\nu_4 + 3\nu_8$ (10.807)
-	10.855	10.857	$5\nu_4$ (10.825)
-	10.877	10.878	$4\nu_4 + 2\nu_8$ (10.867)
-	10.949	10.941	$4\nu_4 + 3\nu_8$ (10.969)
-	10.994	10.980	$6\nu_4$ (10.987)
-	11.018	11.025	$5\nu_4 + 2\nu_8$ (11.029)
-	11.062	11.070	$4\nu_4 + 4\nu_8$ (11.071)
-	11.155	11.160	$7\nu_4$ (11.149)
-	11.217	11.223	$6\nu_4 + 2\nu_8$ (11.191)
-	11.256	11.259	$7\nu_4 + \nu_8$ (11.251)
-	11.283	11.280	$6\nu_4 + 3\nu_8$ (11.293)
-	11.309	11.310	$8\nu_4$ (11.311)
-	11.347	11.346	$7\nu_4 + 2\nu_8$ (11.353)
-	11.404	11.403	$6\nu_4 + 4\nu_8$ (11.395)
-	11.479	11.481	$9\nu_4$ (11.473)
-	11.527	11.532	$8\nu_4 + 2\nu_8$ (11.515)

11.664	11.672	0
11.704	-	$\nu_9$
11.728	11.733	$\nu_8$
11.763	-	$\nu_8 + \nu_9$
11.812	11.814	$\nu_6$
11.856	-	$\nu_6 + \nu_9$
11.871	11.877	$\nu_6 + \nu_8$
11.955	11.955	$2\nu_6$
11.979	-	$2\nu_6 + \nu_9$
12.024	12.030	$2\nu_6 + \nu_8$
(12.053)	-	$2\nu_6 + \nu_a + \nu_9$
(12.097)	-	$3\nu_6$
12.162	-	$3\nu_6 + \nu_8$
-	12.06	$n_{\perp} \rightarrow 4p (n^* = 3.470)$
-	12.25	$n_{\perp} \rightarrow 4d (n^* = 3.825)$
-	12.45	$6a' \rightarrow 4p (n^* = 3.582)$
-	12.65	$6a' \rightarrow 4d (n^* = 3.977)$
-	17.59	$3a' \rightarrow 4p(0)$
-	17.84	$(\nu_1)$
-	18.15	$(2\nu_1)$
-	18.36	$(2\nu_1 + \nu_7)$
-	18.47	$(2\nu_1 + \nu_4)$
-	88.62	$n^* = 3.50-3.64)$
18.741	18.767	0
(18.806)	-	$(\nu_8)$
18.866	-	$\nu_7$
18.886	18.90	$\nu_4$
19.052	19.08	$\nu_1$
19.125	-	$\nu_1 + \nu_8$
19.197	19.24	$\nu_1 + \nu_4$
19.342	-	$2\nu_1$
19.405	19.39	$2\nu_1 + \nu_8$
19.467	-	$2\nu_1 + \nu_7$
19.498	-	$2\nu_1 + \nu_4$

Comparison with photoabsorption spectroscopic data (see preceding work [1]).

The photoelectron spectrum of the sixth band related to the  $\tilde{F}^2A'$  state of  $C_2H_3Cl^+$  is represented in Fig. 5c. This band appears to be fairly complex. An attempt to disentangle the vibrational structure of this band is presented in Table 2. Four vibrational normal modes are at least partially resolved in this band and characterized by wavenumbers of  $2420 \pm 80$ ,  $1170 \pm 80$ ,  $1010 \pm 80$  and  $550 \pm 80$   $cm^{-1}$  successively. To the  $3a'$  orbital ionization should correspond a  $\sigma(CH)$  orbital ionization and therefore the CH group geometry should be more strongly modified. To the  $2420$   $cm^{-1}$  wavenumber should correspond one of the three vibration normal modes involving the  $CH_2$  group, i.e.  $\nu_1$ ,  $\nu_2$  and  $\nu_3$  which are characterized by  $3121$ ,  $3086$  and  $3030$   $cm^{-1}$ , respectively in the neutral ground electronic state [12]. Assuming the  $CH_2$  group being the only involved, the wavenumber of  $2420$   $cm^{-1}$  could be assigned to  $\nu_1$  pure  $CH_2$  stretching vibration. The vibrational mode characterized by  $1170$   $cm^{-1}$  can be assigned to the  $\nu_4$  scissoring mode ( $1608$   $cm^{-1}$  in the neutral molecule [12]) whereas the  $\nu_7$  HCCH deformation mode of  $1030$   $cm^{-1}$  in the neutral molecule could be well suited to be assigned to the  $1010$   $cm^{-1}$  normal mode of the  $\tilde{F}^2A'$  ionic state. Finally the wavenumber at  $550$   $cm^{-1}$  should be identified with the  $\nu_8$  normal mode ( $720$   $cm^{-1}$  in the neutral molecule [12]) and corresponding to the  $CH_2$  rocking with a C-Cl stretching contribution.

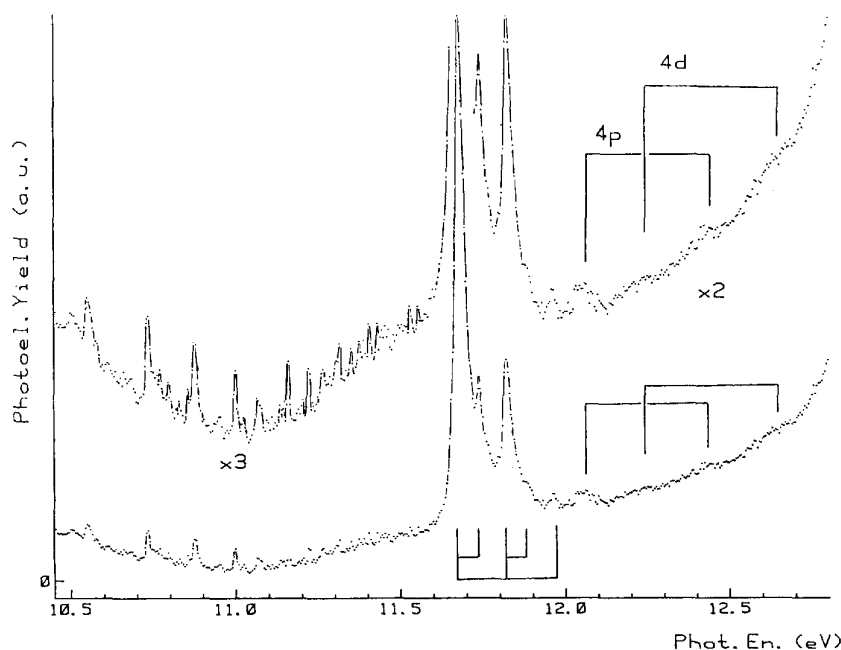
#### 4.1.2. The threshold photoelectron spectrum

As already mentioned in Section 3.1 the most interesting photon energy range starts at 10.013 eV and extends up to about 13 eV. In addition to the vibrational structure observed between 10.013 and 10.5 eV as in the He(I) photoelectron spectrum, numerous sharp features are observed from 10.6 to 11.6 eV. The energy level of these peaks are listed in Table 2. Above this energy, Fig. 2a shows the existence of an underlying and increasing threshold photoelectron signal observed up to 13 eV. In this energy range, displayed in Fig. 6, four diffuse peaks or 'shoulders' have to be mentioned. The position in energy of these structures are listed in Table 2.

Based on the absence of these features in the He(I) photoelectron spectrum, they were ascribed to the probable existence of Rydberg states which have to converge to higher lying ionic states, e.g. those corresponding to  $1a''$  and  $6a'$  ionization.

On the other hand, it has to be mentioned that these four features are regularly spaced by about 200 meV. Two pairs separated by 400 meV could be considered, as shown in Fig. 6. Furthermore, these two pairs could be characterized by effective quantum numbers of about  $n^* = 3.5$  and  $n^* = 3.9$  (see assignment in Table 2), indicating that they possibly pertain to p-type and s/d-type Rydberg series.

**Fig. 6.** Threshold photoelectron spectrum of  $C_2H_3Cl$  in the 10.5-12.8 eV photon energy range. Beside the sharp structures below 11.5 eV and the short vibrational progressions in the  $\tilde{A}^2A'$  state, diffuse structures between 12.0 and 12.7 eV are mentioned and assigned.



The assignments, shown in the fourth column in Table 2, have been obtained as follows. The observed structure must correspond to vibrational levels of the  $C_2H_3Cl^+$  ( $\tilde{X}^2A''$ ) ionic state. According to the geometry variations upon ionization and to the Franck-Condon principle, the  $\nu_4$  and  $\nu_8$  progressions should dominate. Therefore, we have calculated the expected positions of the vibrational levels based on the known wavenumbers, i.e.  $\nu_4 = 1320 \text{ cm}^{-1}$  (0.162 eV) and  $\nu_8 = 820 \text{ cm}^{-1}$  (0.102 eV), and neglecting anharmonicity. The very good agreement obtained between the calculated and observed energies suggests that this assumption holds at least up to  $9\nu_4$  and  $4\nu_8$ .

In the high-energy range of the spectrum, between 17 and 20 eV, the threshold photoelectron spectrum of the  $\tilde{F}^2A'$  ionic state is observed. Below the ionization energy at 18.767 eV a number of weak and broad features are observed and would very likely correspond to Rydberg series converging to the nearest ionization limit. A tentative assignment is proposed in Table 2 where these features should be part of a p-type Rydberg series characterized by an effective quantum number of  $n^* = 3.45 \pm 0.15$  and converging to the  $\tilde{F}^2A'$  state of  $C_2H_3Cl^+$ . The TPES spectrum of the ionic state is made of less numerous and broader structures than in the

corresponding He(I) photoelectron spectrum. Here again the presence of Rydberg states could be responsible for this observation. The position in energy of the structures observed in the threshold photoelectron spectrum is listed in Table 2 together with the tentative assignments.

**Table 3** Energy levels (eV) of the features observed in the CIS spectra related to the  $\tilde{X}^2A''(v_4 = 0-4, 3v_4 + 3v_8)$  vibronic states

CIS- $v_4 = 0$	CIS- $v_4 = 1$	CIS- $v_4 = 2$	CIS- $v_4 = 3$	CIS- $3v_4 + 3v_8$
10.118(w)				
10.180(w)				
	10.284(w)			
	10.314(w)			
	10.424(vw)			
		10.485(w)		
10.513(w)		10.510(w)		
		10.520(w)		
	10.559(w)	10.549(s)		
	10.594(w)	10.590(w)	10.602(w)	
		10.645(w)	10.635(w)	
	10.674(w)			
10.731(vw)	10.734(s)	10.730(vs)	10.730(vs)	
10.761(vw)	10.764(s)	10.765(s)	10.761(w)	
	10.799(w)	10.798(w)	10.790(s)	
	10.829(vw)		10.825(w)	
		10.845(vw)		
	10.874(s)	10.875(s)	10.878(vs)	10.870(vs)
	10.914(w)	10.910(w)	10.915(w)	
	10.949(vw)			10.949(s)
				10.980(vs)
11.008(vw)	10.999(s)	11.000(vs)	11.001(s)	
				11.019(s)
11.070(vw)	11.079(w)	11.015(s)	11.075(s)	
	11.154(w)	11.065(s)		11.109(w)
		11.16(Xw)	11.155(s)	11.154(s)
			11.220(w)	11.219(s)
			11.259(w)	
	11.289(vw)	11.295(w)	11.305(w)	11.309(s)
		11.460(w)		

Intensities are qualitatively described by vw (very weak), w (weak), s (strong) and vs (very strong).

#### 4.2. Constant ion state spectra of $C_2H_3Cl$

Fig. 4a-f displays the CIS spectra of selected vibrational levels of the  $\tilde{X}^2A''$  and the  $\tilde{A}^2A'$  states of  $C_2H_3Cl^+$ . For these curves reflecting the relative photoionization cross-section of the considered vibronic levels, remarkable differences have to be mentioned.

The CIS spectrum of the vibrationless  $\tilde{X}^2A''$  and of the vibrationless  $\tilde{A}^2A'$  vibronic states have very different shape. The former shows the expected behaviour for increasing photon energy. After a steep increase at the onset, the direct ionization cross-section smoothly decreases. A few, very weak autoionization structures could be observed, superimposed on the direct ionization. The latter CIS spectrum, after the steep increase at threshold, shows a shallow minimum followed by a steady increase in the entire observed photon energy range. A trace of the 4p and 4d Rydberg series (see Table 2) could also be observed in this CIS spectrum and marked by vertical bars in Fig. 4f.

The CIS spectra related to the different vibrational levels of the  $\tilde{X}^2A''$  state show a smoothly changing shape when increasing the vibrational quantum number  $v_4$ . Whereas for  $v_4 = 0$  the CIS spectrum is dominated by the smoothly decreasing direct ionization cross-section, for higher vibrational levels the contribution of autoionization markedly increases.

The importance of this contribution (detailed in Table 3) induces an important decrease of the slope between 10.6 and 12.3 eV for  $v_4 = 1$ ,  $v_4 = 2$  and  $v_4 = 3$  and even a plateau is observed for  $v_4 = 1$  and  $v_4 = 2$ . The decrease of the autoionization contribution would be the origin of the fairly sharp ionization cross-section decrease between 11.2 and 11.5 eV and the dip at 11.8 eV observed in these CIS spectra. These features are absent in the CIS spectrum of  $v_4 = 0$ .

The interpretation and assignment of the fine structure detected in the CIS spectra is quite obvious when using the data and assignments listed in Table 2. One is exclusively dealing with autoionization phenomena of Rydberg series converging to the  $\tilde{A}^2A'$ , the  $\tilde{B}^2A''$  and the  $\tilde{C}^2A'$  electronic states, respectively. These spectra very clearly show the dynamics governing the population of the ground vibronic states up to  $v_4 = 9$ . The ionization cross-section systematically reaches nearly zero at about 11.8 eV and higher lying electronic (Rydberg) states very likely contribute to the cross-section increase observed for photon energies above 12.0 eV. This is clearly shown in Fig. 4b and c.

## 5. Conclusions

Together, the photoabsorption spectroscopy [1], the threshold photoelectron (TPES) spectroscopy and the CIS spectroscopy are very powerful techniques for the detailed investigation of the direct ionization and autoionization taking place in a molecular system. These methods have been applied to simple molecules [6]. The present work showed the suitability of these methods to investigate in detail more complex molecular systems, e.g.  $C_2H_3Cl$ .

In this latter case a reinvestigation of the photoabsorption spectrum allowed us to extend the analysis and assignments to higher energies, i.e. to the second ionization limit (see preceding paper [1]). This data analysis appears to be most important to examine the TPES- and CIS spectra. The excitation of several previously unobserved vibrational normal modes, confirmed in a high-resolution He(I) photoelectron spectrum, is put forward. Sharp but weak features, assigned to autoionization, are identified and assigned in both TPES- and CIS spectra.

## Acknowledgements

We are indebted to the University of Liège, the FRFC (Fonds de la Recherche Fondamentale Collective), the Freie Universität Berlin and the Bundesministerium für Forschung und Technologie for financial support. RL and BL acknowledge the European Community for financing this work through its Human Capital and Mobility Programme (Contract No. CHGE-CT93-0027). We wish to thank the BESSY technical Staff, and particularly Dr. G. Reichardt, for the outstanding quality of the maintenance of the equipment.

## References

- [1] R. Locht, B. Leyh, K. Hottmann, H. Baumgärtel, *Chem. Phys.* 220 (1997) 207.
- [2] R. Kaufel, Ph.D. Thesis, Freie Universität Berlin, Berlin (1985).
- [3] G. Tornow, Ph.D. Thesis, Freie Universität Berlin, Berlin (1986).
- [4] K. Wittel, H. Bock, *Chem. Ber.* 107 (1974) 317.
- [5] K. Hottmann, H.-W. Jochims, H. Baumgärtel, *BESSY Jahresber.* (1987) 398.
- [6] E.W. Plummer, T. Gustafsson, W. Gudat, D.E. Eastman, *Phys. Rev. A* 15 (1977) 2339.
- [7] R.F. Lake, H. Thompson, *Proc. R. Soc. London, Ser. A* 315 (1970) 323.
- [8] W. Von Niessen, L. Åsbrink, G. Bieri, *J. Electron Spectrosc. Relat. Phenom.* 26 (1982) 173.
- [9] K.H. Sze, C.E. Brion, A. Katrib, B. El-Issa, *Chem. Phys.* 137 (1989) 369.
- [10] D. Reinke, R. Krässig, H. Baumgärtel, *Z. Naturforsch., Teil A* 28 (1973) 1021.
- [11] Dewar Research Group: the AMPAC package (containing the MNDO/3, MNDO and AM1 methods), Chemistry Department, University of Texas, Austin, TX 78712. The package was converted for an IBM3090 computer by R. Farren and E.R. Davidson, Department of Chemistry, Indiana University, Bloomington, IN 47405, and is distributed by the Quantum Chemistry Program Exchange under reference

*Published in: Chemical Physics (1997), vol. 220, pp. 217-232.*  
*Status: Postprint (Author's version)*

number 539.

[12] G. Herzberg, Molecular Spectra and Molecular Structure, III. Electronic Spectra and Electronic Structure of Polyatomic Molecules, D. van Nostrand, Princeton, NJ, 1967.